Fisetin derivatives exhibit enhanced anti-inflammatory activity and modulation of endoplasmic reticulum stress

Daniela Correia da Silva[1], Peter J. Jervis[2], José A. Martins[2], Patrícia Valentão[1], Paula M. T. Ferreira[2], David M. Pereira[1]*

[1]*REQUIMTE/LAQV, Laboratório de Farmacognosia, Departamento de Química, Faculdade de Farmácia, Universidade do Porto, Rua de Jorge Viterbo Ferreira, Nº 228, 4050-213, Porto.*

[2]*Chemistry Centre, School of Sciences, University of Minho, 4710-057 Braga, Portugal;*

Abstract: Fisetin (FST) is a dietary flavonol that is known to possess multiple relevant bioactivities, raising the question of its potential health benefits and even its use in novel pharmacological approaches. To attain this prospect, some limitations to this molecule, namely its poor bioavailability and solubility, must be addressed.

Inflammation and endoplasmic reticulum (ER) stress are often hand in hand in the context of chronic disease. Both are activated upon perceived disturbances in homeostasis but can be deleterious when intensely or chronically activated. We have synthesized a set of FST derivatives trying to improve the biological properties of the parent molecule. These new molecules were tested along with the original compound for their ability to mitigate the activation of these signaling pathways.

FST has proven to be effective against the onset of inflammation, reducing NF-κB activation, cytokine release, inflammasome activation and ROS generation, as well as decreasing the activation of the unfolded protein response (UPR). Some of the tested derivatives are also described as new caspase-1 inhibitors, being also capable of reducing pro-inflammatory cytokines and ER stress markers.

Keywords: fisetin, natural products, IL-6, TNF-α, IL-1β, ATF4, CHOP

Corresponding author: dpereira@ff.up.pt

1. Introduction

Inflammation encompasses the activation of several signaling cascades and recruitment of specialized cells in an attempt to restore homeostasis upon the detection of danger signals, either arising from injury or infection. Chronic activation of inflammatory signaling is known to underlie chronic diseases [1].

The endoplasmic reticulum (ER) is in charge of protein synthesis and folding of a substantial portion of the proteome of eukaryotes. The complexity of this process renders it error prone, and thus this organelle relies on signaling pathways to detect misfolded/unfolded protein in the ER lumen and attempt to restore homeostasis. These signaling pathways are known as the unfolded protein response (UPR) [2]. Even though both inflammation and UPR signaling have evolved to promote cell survival, both can be deleterious. In fact, both chronically activated in the context of chronic diseases [3, 4].

The flavonol fisetin (FST), or 3,3',4',7-tetrahydroxyflavone was first isolated from *Rhus cotinus* L., commonly known as venetian sumac, in 1833, and its chemical structure was elucidated near the end of the century [5]. It is synthesized as a secondary metabolite in multiple plants, including common plants in our diet, such as strawberries (160 µg/g), apples (26.9 µg/g), persimmons (10.6 µg/g), onions (4.8 µg/g), grapes (3.9 µg/g) and kiwis (2.0 µg/g), occurring in leaves, stems, barks, hardwoods and fruits [5, 6].

The average dietary intake of FST is estimated at 0.4 mg/day in geographies where this information is available, namely the Japanese population [7]. Dietary supplements containing FST are available in the market, and are advertised as conveyers of multiple health benefits due to the bioactivities mentioned herein and the ability of this molecule to cross the blood-brain-barrier [8]. Even though no FST-based products are used for pharmacological purposes [5], there are several ongoing clinical trials, including phase III clinical trials (NCT05482672, NCT05505747).

FST has been widely studied recently, and it has been proven to possess multiple relevant bioactivities [6]. One example is its capacity to scavenge free radicals. This antioxidant potential is thought to be owed to the *o*-dihydroxy structure in the B ring and the 3-hydroxy group and 2,3-double bond in the C ring contribute to the antioxidant activity of FST [6]. This molecule has a possible therapeutic effect against cancer by exerting antiproliferative and apoptotic effects, as well as modulating key signaling pathways such as NF-κB and MAPK [9-11]. FST has been described as neuroprotective by being antioxidant and anti-inflammatory, as well as increasing intracellular glutathione levels and promoting synaptic plasticity [8, 12-14]. Furthermore, it is described as being capable of modulating ER stress response, resulting in decreased protein aggregation under stress conditions [15]. Relevantly, FST has shown promise in areas such as neurodegeneration and cancer, that implicate both inflammation and ER stress signaling.

Low solubility in water and poor bioavailability may be limiting the use of this molecule in the pharmacological context [9, 16]. For this reason, it is important to tailor this molecule into safer, more stable and active derivatives that can aid in the development of FST-based pharmacological strategies and also add to the current understanding of its bioactivities. In this work, we describe the bioactivity of several novel synthetic FST derivatives in the context of inflammatory and ER stress signaling. The discoveries published herein may contribute to provide new modulators of both signaling pathways into the current pharmacological arsenal.

2. Materials and Methods

2.1. Synthesis

FST derivatives FST1–7 were synthesized using methods developed in our laboratory, as outlined in Scheme 1. The experimental procedures and characterization

77 data for the compounds FST1–7 are presented in the Supplementary Material. FST was
78 acquired from the Abcam chemical company (Cambridge, UK). All other reagents were
79 purchased from Sigma-Aldrich or Acros and used without further purification. Analytical
80 grade solvents were used, and dried by standard methods when required. Distilled water
81 was used when aqueous medium was needed. Reactions were monitored by thin layer
82 chromatography (TLC) on Merck-Kieselgel plates 60 F254 and detection was made by
83 examination under UV light (240 nm) or by adsorption of iodine vapour.
84 Chromatographic separations were performed on silica MN Kieselgel 60 M (230–400
85 mesh). NMR spectra were acquired on a Bruker Avance III 400 spectrometer. NMR
86 spectra were recorded at 25 °C, using the residual solvent signals as reference. Deuterated
87 dimethyl sulfoxide (DMSO-d_6) and deuterated chloroform ($CDCl_3$) were used as
88 solvents. Chemical shifts are given in parts per million (ppm) and the coupling constants
89 in Hertz (Hz). Mass spectrometry data were recorded by a ThermoFinnigan LxQ (Linear
90 Ion Trap) mass detector with electrospray ionisation (ESI).
91

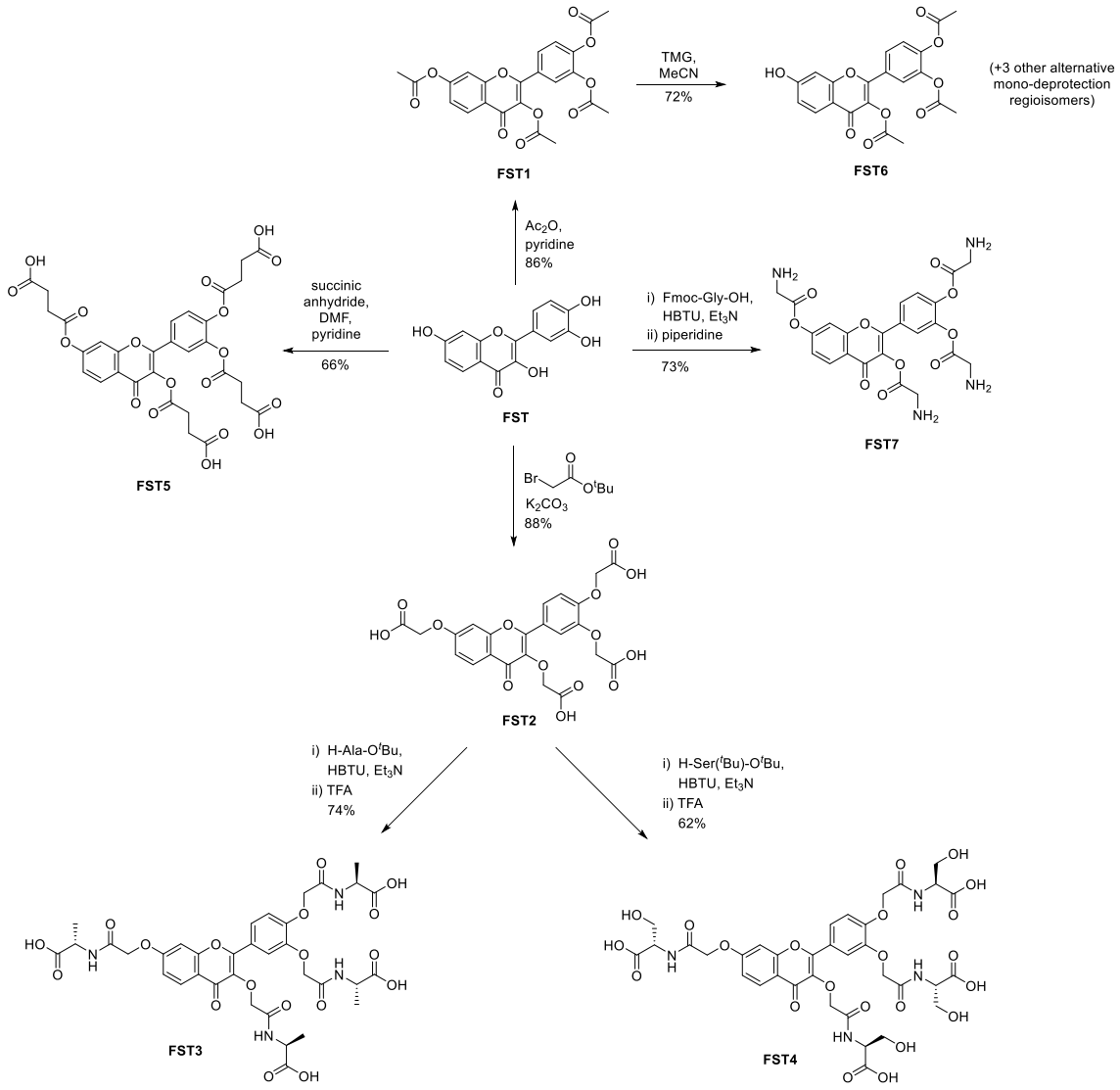

Scheme 1. Synthetic routes to FST derivatives (FST1-7).

2.2. Cell culture conditions

THP-1 and THP-1 Lucia™ NF-κB monocytes were cultured at 37 ºC with 5% CO_2, in RPMI 1640 medium, with 10% FBS, 1% penicillin/streptomycin and HEPES at 25 mM. Additionally, as recommended by the supplier, medium for THP-1 Lucia™ NF-κB monocytes contained 100 μg/mL Normocin™. Zeocin™ (100 μg/mL) was included every other passage to ensure selective pression.

2.3. MTT reduction assays

Cellular viability was inferred according to the results of MTT reduction assays, carried out in 96-well plates. In these plates, THP-1 monocytes were seeded at a density of 6 x 10^4 cells/well. Differentiation of monocytes into macrophages was promoted with the addition of PMA at 50 nM when seeding. Medium contained PMA was discarded and replaced with fresh medium after 24 h. In the following day, differentiated macrophages were incubated with the solutions containing the molecules under analysis. After 24 h of incubation with the compounds, the medium was replaced with MTT at 0.5 mg/mL and incubated for 2 h. At this point, the MTT solution was discarded. The resulting crystals were dissolved in a 3:1 DMSO:isopropanol solution. Finally, the absorbance at 560 nm was read in a Thermo Scientific™ Multiskan™ GO microplate reader.

2.4. NF-κB activation assay

A luciferase based-assay was employed to determine the translation levels of the NF-κB transcription factor. The seeding of THP-1 Lucia™ NF-κB monocytes was performed as described above for the MTT reduction assays. 2 h after the incubation with the molecules of interest, LPS (from *E. coli*) was added at the final concentration of 1 µg/mL, in all wells except for the control group, promoting polarization of the macrophages into their pro-inflammatory phenotype, or M1. 24 h after the incubation with compounds, or 22 h after the addition of LPS, 20 µL of medium from each well was transferred to a clean 96-well plate, where 50 µL of QUANTI-Luc™ substrate solution was added each well, as according to the instructions from the supplier. The plate was shaken, and luminescence was immediately read in a Cytation™ 3 (BioTek) microplate reader.

2.5. Pro-inflammatory cytokine release by ELISA

As described for the previous assays, THP-1 macrophages were seeded and differentiated in 96-well plates. After differentiation, cells were incubated with molecules of interest and LPS at 1 µg/mL was added after 2 h. Supernatants were collected 22 h after the addition of LPS. Concentrations of TNF-α, IL-6 and IL-1β were determined in the supernatant samples by ELISA. A specific kit for each cytokine was acquired, and the manufacturer's instructions (BioLegend Inc.; San Diego, CA, USA) were followed.

2.6. Quantification of ROS generation

THP-1 monocyte seeding was carried out as in the previous assays, only in black-bottomed 96-well plates. The molecules were once again incubated for a period of 24 h, including 22 h in the presence of LPS at 1 µg/mL. At this point, a washing step with HBSS ensued, followed by incubation with the fluorescent probe DCFH-DA at 25 µM for 30 min, in HBSS. Fluorescence at 490/520 nm was read in a Cytation™ 3 (BioTek) microplate reader.

2.7. Caspase-Glo® 1 Inflammasome Assay

Cells were seeded as mentioned above, only in white-bottomed 96-well plates. After the addition of LPS at 1 µg/mL, the incubation period was of 90 min. According to the instructions from the supplier, after these 90 min, Caspase-Glo® 1 Reagent was added to each well, in the absence and presence of the selective caspase-1 inhibitor Ac-YVAD-CHO, following a period of 60 min of incubation at room temperature. Finally, luminescence was read on a Cytation™ 3 (BioTek) microplate reader.

2.8. RNA extraction, quantification, conversion and RT-qPCR

In order to obtain mRNA samples, THP-1 monocytes were seeded in 12-well plates at a density of 4.8 x 10^5 cells/well. The compounds were incubated after differentiation of the monocytes into macrophages, as mentioned above. LPS was added after 2 h, and the plates were left in the incubator for 16 h. At this point, samples were obtained by resorting to the PureZOL RNA isolation reagent. RNA extraction was performed by phase separation, according to the instructions provided by the supplier. After the extraction, RNA in the sample was quantified with the Qubit® RNA HS assay kit. The conversion to cDNA, using 1 µg of sample, was performed using the SuperScript™ IV VILO™ MasterMix. Our primers (**Table 1**) were designed on Primer BLAST (NCBI, Bethesda, MD, USA) and purchased to Thermo Fisher (Waltham, MA, USA).

The reaction was conducted with KAPA SYBR® FAST qPCR Kit Master Mix (2X) Universal, and took place in a qTOWER3 G (Analytik Jena AG, Germany), in the following conditions of thermal cycling: 3 min at 95 ºC, followed by 40 cycles of 95 ºC for 3 s (denaturation), gene-specific temperature for 20 s (annealing), and 20 s at 72 ºC (extension). Melting curves were observed to guarantee product specificity. Gene expression was normalized against the reference gene *gapdh*. Data was analyzed in the qPCRsoft 4.0 software, supplied with the equipment.

Table 1. Analyzed genes, NCBI accession numbers, primers, annealing temperatures and amplification product size.

Gene	Accession number	Primers	Annealing Temperature (ºC)	Amplicon length (bp)
Gapdh (GAPDH)	NM_002046.6	F: AGGTCGGAGTCAACGGATTT R: TGGAATTTGCCATGGGTGGA	60	157
Ddit3 (CHOP)	NM_001195053.1	F: AAGTCTAAGGCACTGAGCGT R: TTGAACACTCTCTCCTCAGGT	59	93
Atf4 (ATF4)	NM_001675.4	F: ACAACAGCAAGGAGGATGCC R: CCAACGTGGTCAGAAGGTCA	60	135
Edem1 (EDEM1)	NM_014674.2	F: GCGGGGACCCTTCAAATCT R: CGGCTTTCTGGAACTCGGAT	60	117

2.9. Tanimoto coefficient

All molecules were drawn in RdKit having their SMILES strings as input. For the calculation of Tanimoto coefficients, SMILES were used to calculate extended-connectivity fingerprints (ECFP4) fragments which were then used as input for the calculation of Tanimoto coefficients in a pairwise fashion with FST, using the formula:

$$SIM_{AB} = \frac{c}{a + b - c}$$

in which ***c*** bits set in common in the two fingerprints and ***a*** and ***b*** are bits set in the fingerprints for molecules **A** and **B.**

2.10. Statistical analysis

GraphPad Prism 8 software was utilized for the statistical analysis, namely to perform unpaired Student's t-test to compare single treatments with control groups, with values of $p < 0.05$ considered statistically significant. Furthermore, outliers were detected with the Grubbs' test.

3. Results and Discussion

3.1. Synthesis of FST derivatives

The parent molecule fisetin (FST) and the derivatives synthesized (FST1–7) can be found in **Fig. 1**. We also calculated a number of molecular and topographical descriptors that can be found in **Table 2**.

In order to assess the degree of chemical divergence introduced by the modifications conducted, we calculated the Tanimoto coefficient for all derivatives obtained having FST as reference molecule.

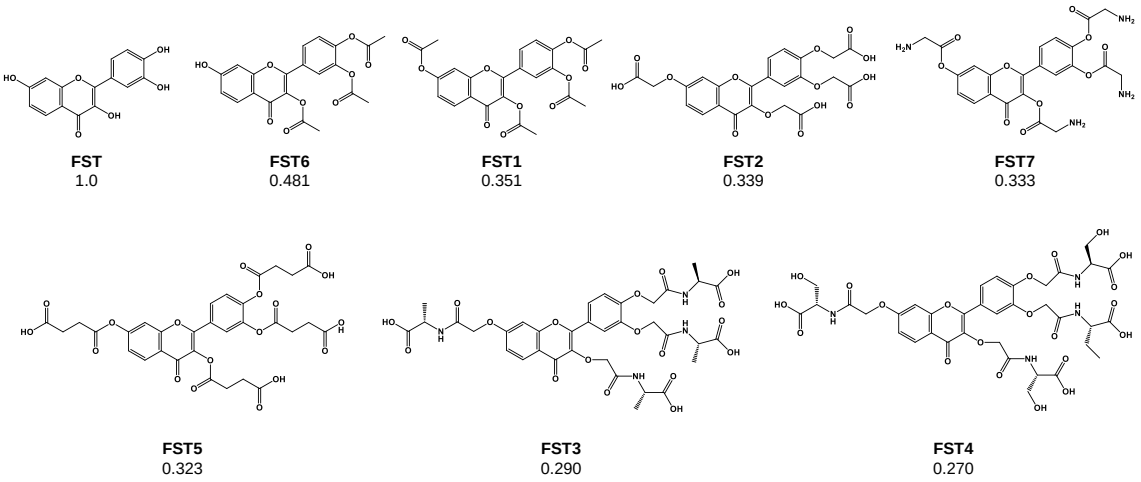

Fig. 1. FST derivatives sorted according to their Tanimoto coefficient calculated using RdKit. FST was used as a reference molecule for pairwise calculation of the coefficient.

As shown in **Fig. 1**, FST6 is the closest molecule to the parent compound FST, followed by FST1 and FST2. FST3 and FST4 are the more chemically divergent molecules, owing not only to their complexity but also to the nature of their substituents. In fact, the BertzCT descriptor, which aims to quantify the complexity of a molecule, as expected, presents the highest values of the library for FST3 and FST4 (2114.7 and 2189.6, respectively, against 909.9 of FST, **Table 2**).

Table 2. Molecular and topographical descriptors of FST and derivatives.

Molecule	FST	FST1	FST2	FST3	FST4	FST5	FST6	FST7
MaxEStateIndex	12,08	13,07	13,15	13,85	13,91	13,57	12,87	13,23
MinEStateIndex	-0,65	-0,77	-1,38	-1,35	-1,74	-1,34	-0,75	-0,94
MaxAbsEStateIndex	12,08	13,07	13,15	13,85	13,91	13,57	12,87	13,23
MinAbsEStateIndex	0,09	0,04	0,03	0,00	0,00	0,17	0,03	0,01
qed	0,51	0,42	0,25	0,07	0,04	0,12	0,51	0,20
MolWt	286,24	454,38	518,38	802,70	864,72	686,53	412,35	514,45
NumValenceElectrons	106	170	194	306	330	258	154	194
MaxPartialCharge	0,23	0,31	0,34	0,33	0,33	0,31	0,31	0,32
MinPartialCharge	-0,51	-0,45	-0,48	-0,48	-0,48	-0,48	-0,51	-0,45
MaxAbsPartialCharge	0,51	0,45	0,48	0,48	0,48	0,48	0,51	0,45
MinAbsPartialCharge	0,23	0,31	0,34	0,33	0,33	0,31	0,31	0,32
BalabanJ	2,34	2,27	2,16	2,10	2,12	2,15	2,28	2,24
BertzCT	909,92	1349,34	1420,95	2114,71	2189,64	1885,01	1237,19	1433,03
Kappa1	12,86	23,19	26,34	44,01	47,86	36,87	20,59	26,97
Kappa2	4,45	9,35	11,44	19,79	22,59	16,82	8,08	11,87
Kappa3	2,02	5,42	6,88	12,86	13,79	11,31	4,30	6,33
TPSA	111,13	135,41	216,33	332,73	393,42	284,61	129,34	239,49
FractionCSP3	0,00	0,17	0,17	0,34	0,36	0,26	0,14	0,17
MolLogP	2,28	3,16	1,31	-0,67	-3,36	2,54	2,94	-1,08
MolMR	74,58	113,16	120,44	190,86	199,71	157,94	103,51	126,68

3.2. Impact of fisetin derivatives on macrophage cell viability

THP-1 monocytes, when differentiated into M1 macrophages, are frequently used to assess the anti-inflammatory potential of small molecules, given their high expression pattern of relevant receptors such as the toll-like receptor 4 (TLR4) [17].

This work began with the evaluation of the cytotoxic effect of FST and its 7 derivatives in order to define the highest concentrations that could be safely used in this experimental model without impacting cell viability. It is clear on **Fig. 2** that FST and FST7 present the highest cytotoxicity, exerting a statistically significant effect from 25 µM. Two more molecules, FST1 and FST2, were cytotoxic at 50 µM. On the other hand, FST3, FST4, FST5 and FST6 were not cytotoxic up to 50 µM. In subsequent assays, the

two highest nontoxic concentrations of each compound were used, in order to observe the strongest possible effect of FST and derivatives without compromising cell viability.

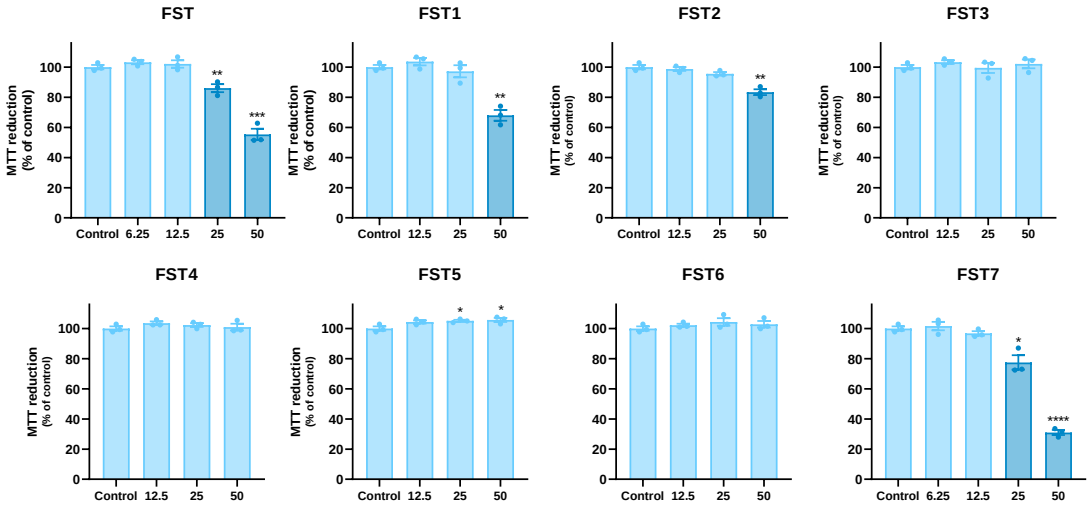

Fig. 2. Effect of FST and each derivative upon cell viability of THP-1 macrophages after 24 h of incubation, determined by MTT reduction assays. Results as percentage of the control correspond to the mean ± SEM of three independent experiments, individually conducted in triplicate.

3.3. FST and derivatives inhibit LPS-mediated NF-κB activation

NF-κB is a transcription factor that, upon activation, induces the expression of multiple pro-inflammatory cytokines and chemokines, while also resulting in inflammasome assembly [18]. As a major regulator of the inflammatory response, it was chosen as a target to an initial evaluation of the anti-inflammatory potential of FST and derivatives. To this end we used THP-1 monocytes transfected with a NF-κB-inducible luciferase reporter construct (THP1-Lucia™ NF-κB), allowing the determination of NF-κB activation levels.

The results show that FST derivatives FST4, FST5 and FST6 did not display any capacity to inhibit NF-κB signaling in LPS-challenged macrophages in any of the

concentrations tested (**Fig. 3**). For this reason, these three derivatives were dropped from the study and were not tested in the subsequent experiments. The parent compound, FST, as well as derivatives FST1, FST2, FST3 and FST7 were all remarkably effective at inhibiting the activation of NF-κB under our experimental conditions, being active in all tested concentrations. FST7 displays over 50% of inhibition at a concentration as low as 6.25 µM, thus being more active than the parent molecule. The same occurs with FST1 at 12.5 µM. The lowest concentration of FST3 results in NF-κB signaling near the basal levels, the most potent activity recorded for any of the derivatives.

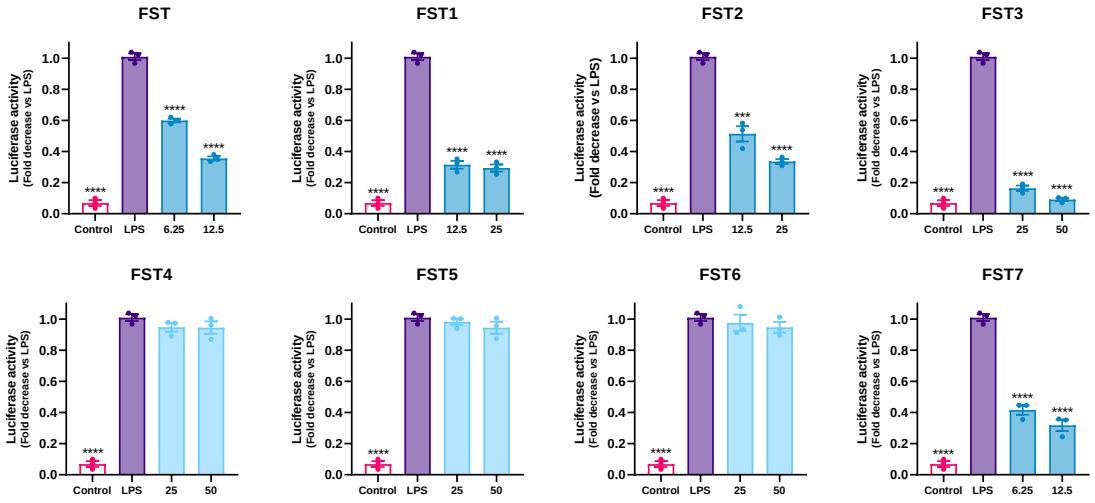

Fig. 3. Effect of the two highest nontoxic concentrations of each molecule under study upon NF-κB activation after 22 h of LPS exposure, determined by the QUANTI-Luc™ luciferase activity assay in THP-1 Lucia™ NF-κB. The presented results express the relative NF-κB when compared to the positive control, including the mean ± SEM of three independent experiments, individually performed in duplicate.

When examining the properties of the 3 molecules dropped due to lack of activity (FST 4-6), it is clear that they exhibit the most extreme values of logP (FST4: -3.36, FST5: 2.54, FST6: 2.94), apart from FST1. In the case of the latter, it could be the case that the logP value of 3.16, the highest among all molecules tested, is relevant to the activity of the molecule.

3.4. FST and some derivatives inhibit ROS generation

The activation of NF-κB and other signaling pathways is a hallmark of M1 macrophage activation, as well as increased expression of proteins such as the matrix metalloproteinases (MMPs), induced expression of pro-inflammatory cytokines like TNF-α, IL-1α, IL-1β, IL-6, IL-12, IL-18, and IL-23, generation of nitric oxide (NO), reactive nitrogen species (RNS) and reactive oxygen species (ROS) [19].

ROS are particularly well-established mediators of initiation, progression and resolution of inflammation. The oxidative burst is a broadly known phenomenon that results from the extensive phagocytosis of pathogens and cell debris performed by neutrophils and macrophages that are recruited towards the inflammation site [20]. Therefore, it is relevant to analyze what occurs at the level of ROS generation by the action of the NF-κB signaling inhibitors that we identified in the previous assay.

Here we evaluated the ability of the molecules that had displayed anti-inflammatory potential in the previous assay to inhibit excessive ROS generation caused by LPS. FST significantly inhibited ROS production only in the highest tested concentration (12.5 µM), the same being true for FST7 (**Fig. 4**). FST1, even though inactive at 12.5 µM, was also effective in its respective highest tested concentration (25 µM), displaying a stronger effect than that of FST and FST7. FST3 was the molecule displaying the stronger effect, reaching over 50% of inhibition at the highest tested concentrations. Even though the tested concentrations were higher (25 and 50 µM), both were observed before as not impactful towards cell viability, which, as hypothesized above, may explain why we were able to achieve a higher inhibition with this molecule.

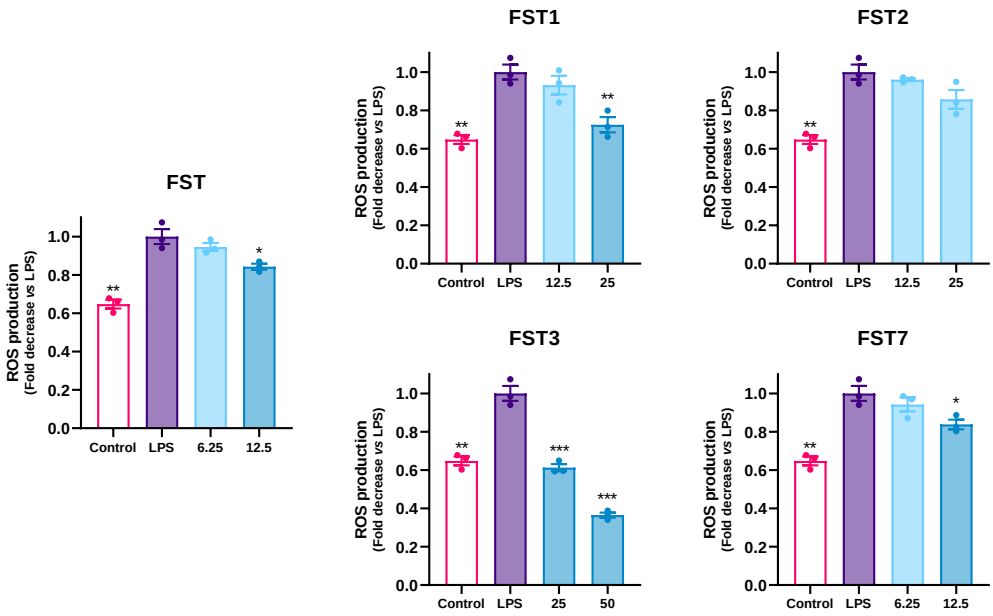

Fig. 4. Impact of two highest concentrations of anti-inflammatory molecules on the generation of ROS by LPS-insulted THP-1 macrophages, determined by the fluorescence of DCFH-DA. Results express mean ± SEM of three independent experiments carried out in triplicate.

3.5. FST and its derivatives decrease caspase-1 activation

The NLRP3 (NOD-, LRR- and pyrin domain-containing protein 3) inflammasome is a multimeric protein complex that consists of the innate immune receptor NLRP3, the adaptor protein ASC (apoptosis-associated speck-like protein containing CARD [caspase recruitment domain]) and the inflammatory caspase-1. Proteolytic cleavage of procaspase-1 in the inflammasome renders the active form of the protease. This event is used in this assay as a means to assess the activation of the NLRP3 inflammasome, that is known to be induced in the presence of microbe ligands, such as LPS, and result in caspase-1 activation and consequent cleavage of pro-IL-1β and release of its active form [21]. Furthermore, NLRP3 inflammasome activation is one of the bridges connecting inflammatory and ER stress signaling, since it is known to mediate ER stress-induced inflammation [22]. It is then justified to determine the ability of the molecules displaying

an anti-inflammatory potential to impact caspase-1 activity, and, indirectly, on NLRP3 inflammasome activation.

The results obtained show that every molecule under analysis was capable of inhibiting caspase-1 activation in its highest tested concentration. In fact, the parent compound FST has already been described as inhibitor of caspase-1 expression, as well as of IL-1β secretion *in vivo* [23]. Only two molecules were effective at inhibiting NLRP3 inflammasome activation in both tested concentrations, specifically FST1 and FST3 (**Fig. 4**). Being that the inhibition rate is somewhat similar in both of these molecules, it can be argued that FST1 is the most effective molecule for this purpose, given that the tested concentration is lower.

Relevantly, NLRP3 inflammasome activation is often triggered by ER stress and UPR activation, deeming UPR modulation and NLRP3 inhibition a possible strategy to relieve inflammation [24]. Currently, there are no approved drugs to modulate NLRP3 [25] or caspase-1 [26], since few molecules have entered clinical trials and they have failed. The need for modulators of inflammasome activation that are of low toxicity remains, and FST and derivatives are promising molecules to attain this goal. With our results, we expand the chemical space for which caspase-1 inhibitors are known.

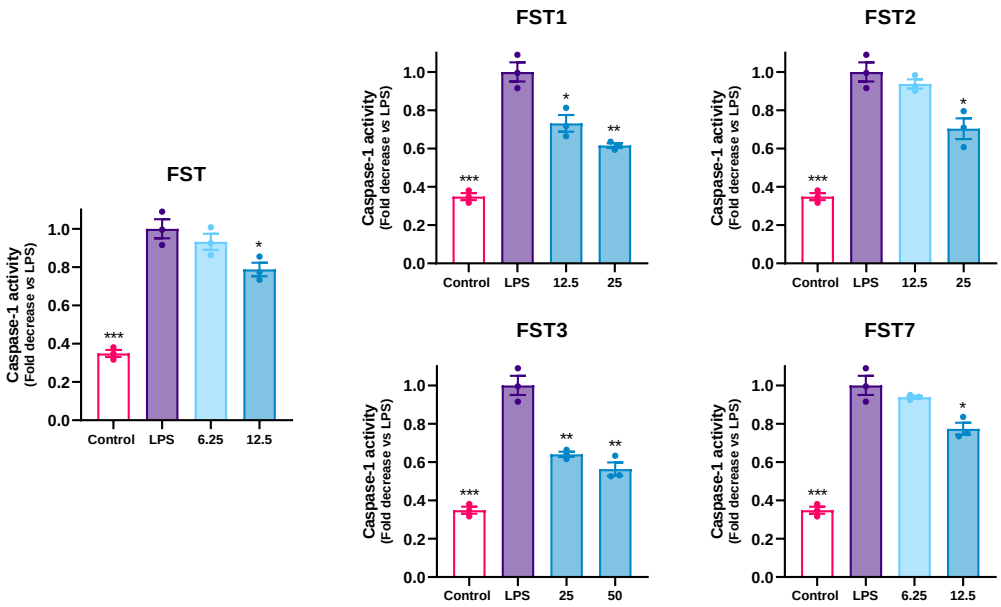

Fig. 4. Effect of anti-inflammatory molecules on LPS-induced caspase-1 activation on THP-1 macrophages. Proteolytic activation of caspase-1 indicates NLRP3 inflammasome activation. Results are expressed as fold decrease *versus* maximum activation (on LPS-challenged cells) and stand for the mean ± SEM of three independent assays, with each performed in duplicate.

3.6. FST and derivatives inhibit LPS-induced pro-inflammatory cytokine production

Immune cells, notably macrophages, recognize an infection through its pathogen-recognition receptors (PRRs), such as TLRs. Following NF-κB activation, the synthesis and release of pro-inflammatory mediators ensues, including the cytokines IL-6, TNF-α and IL-1β [27, 28]. These three major cytokines, despite possessing potentially both pro- and anti-inflammatory properties, are mainly pro-inflammatory cytokines secreted by activated M1 macrophages, being involved in the modulation of the acute phase response [19, 29]. We assessed the impact of all molecules under study upon the production of these cytokines, with the steroid anti-inflammatory drug dexamethasone being used as a positive control for the inhibition of their release.

Regarding the potential of FST and derivatives to inhibit LPS-induced IL-6 release, it is displayed in **Fig. 5** that all tested FST derivatives significantly inhibit IL-6 release in both tested concentrations. FST is the only molecule under analysis that was effective only in the highest tested concentration. In the case of TNF-α, even though every molecule has shown to be active (**Fig. 5**), the inhibitory potential was lower than in the case of IL-6. All molecules were effective at their highest tested concentration, while only FST3 was effective in both concentrations. This molecule was also the only capable of displaying any significant inhibition of IL-1β, albeit only at 50 μM (**Fig. 5**).

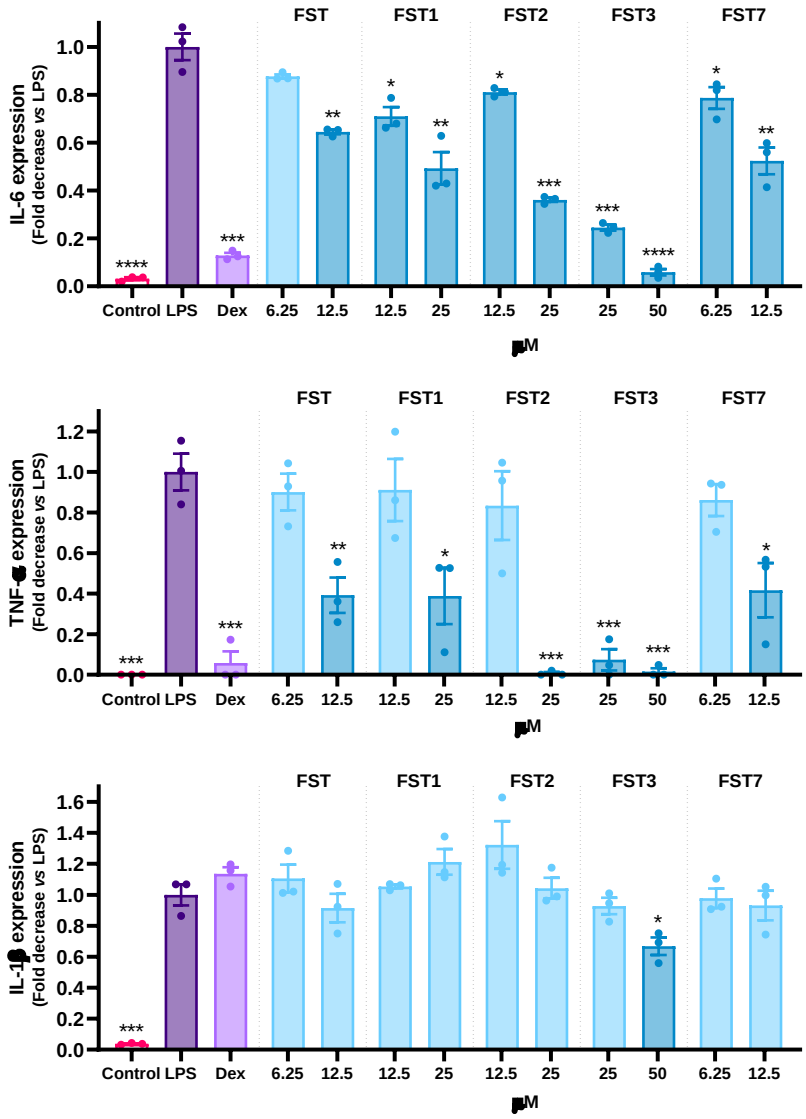

Fig. 5. Influence of active molecules on the protein expression of the pro-inflammatory cytokines IL-6, TNF-α and IL-1β, as determined by ELISA. Results presented fold decrease against maximum activation, and represent the mean ± SEM of at least three independent experiments, individually performed in triplicate.

3.6. Anti-inflammatory effect of FST and derivatives is concomitant with ER stress attenuation

ER stress and the UPR activation the follows result in the enhanced expression of a battery of genes. Therefore, the evaluation of the transcriptional outcome at the level of ER stress in the presence of LPS and the compounds of interest was assessed. The *edem1* gene encodes the EDEM1 (ER degradation enhancing-mannosidase-like protein), an

important enzyme in ER-associated degradation (ERAD) of misfolded proteins [30]. The *atf4* gene encodes the ATF4 (activating transcription factor 4). This is a transcription factor that induces, among others, the expression of protein folding-related genes. Its expression is selectively enhanced upon UPR activation, that also being the case of *ddit3*. The translation of the latter results in the CHOP (CCAAT-enhancer-binding protein homologous protein) transcription factor, that governs processes of ER stress-induced regulated cell death [31]. These three UPR-related genes saw their expression increased by incubation with LPS, as evidenced in **Fig. 6**.

FST resulted in significant inhibition of the LPS-induced overexpression of *edem1*. FST7 also exhibited a mild effect on this gene, while FST3 exerted a more pronounced effect. This indicates that ERAD is decreased, and thus ER stress is ameliorated.

Notably, regarding *ddit3*, every molecule was effective. Apart from FST1, which was still effective in the highest tested concentration, every molecule significantly inhibited LPS-induced overexpression of *ddit3* in a statistically significant manner in both tested concentrations, attesting for the ability of FST and derivative compounds to reduce inflammation while restoring ER homeostasis. Increased *ddit3* expression is classically attributed to PERK/ATF4 signaling, but this gene is a downstream target of every UPR signaling branch, including ATF6 and IRE1/XBP1 [32]. CHOP is a pro-apoptotic transcriptional factor, and thus the fact that every molecule inhibits its overexpression attests for their potential to preserve cellular homeostasis upon LPS insult [33]. Similarly to what was observed in other evaluated parameters, FST3 was the molecule that displayed the most promising potential.

FST and its derivative compounds failed to restore the expression levels of *atf4* to basal levels, even FST3 at 50 µM, that was active in every other parameter analyzed. However, even though the mRNA levels did not decrease, ATF4 activation may be decreased. This

could explain the enhanced mRNA expression of this transcription factor at this point. Furthermore, the activation and translocation to the nucleus of this transcription factor has been observed to be induced by TLR4 signaling in a JNK-dependent manner. ATF4 promotes inflammation by positively regulating the secretion of cytokines like IL-6. Furthermore, TLR4 signaling leads to increased protein stability of this protein [34]. TLR4 signaling is decreased by effect of FST and derivatives, further adding to the hypothesis that ATF4 activation may be decreased independently of its mRNA levels.

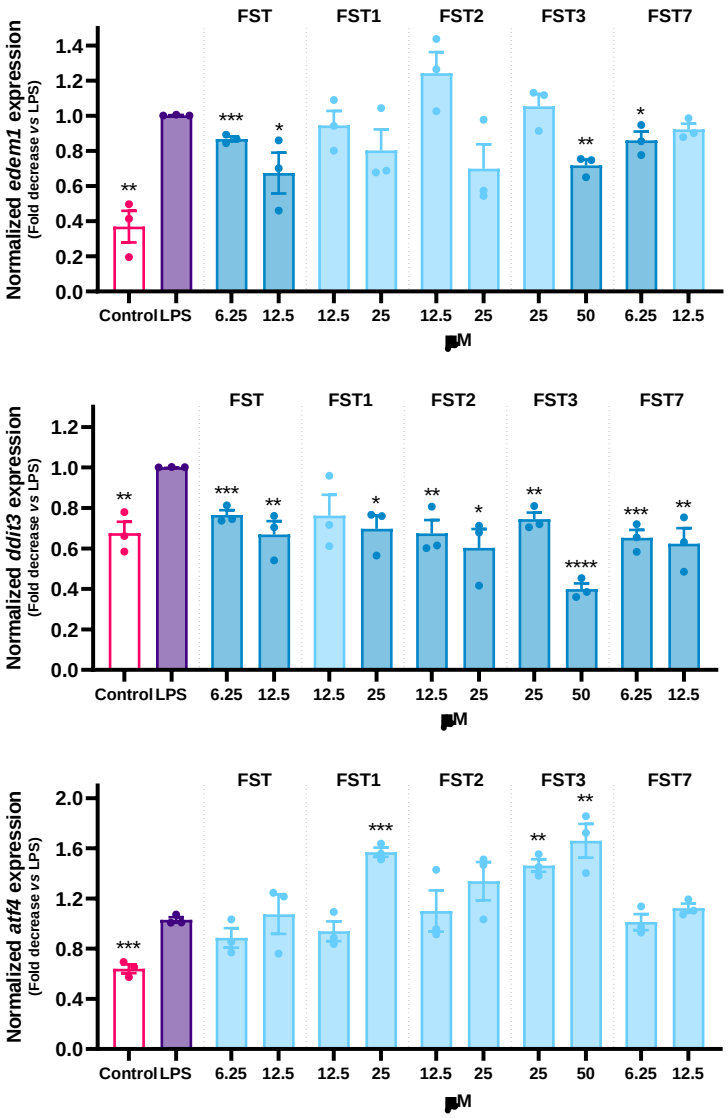

Fig. 6. Effect of the anti-inflammatory molecules on gene expression of UPR target genes, namely *edem1*, *ddit3* and *atf4*, evaluated by RT-qPCR. Gene expression was normalized

against *gapdh*. The results display the mean ± SEM of three independent assays, with each individually conducted in duplicate.

4. Conclusions

Despite its wide coverage in scientific literature, the biological activities of fisetin have yet to be present in therapeutic approaches for any type of disease.

FST has significantly attenuated LPS-induced onset of inflammation and ER stress, simultaneously ameliorating NF-κB activation, ROS generation, pro-inflammatory cytokine release, capase-1 and, consequently, inflammasome activation. Concurrently, FST impaired activation of the UPR triggered in response to LPS, as observed by the decreased gene expression of target genes. Relevantly, FST and all its derivatives that could inhibit NF-κB signaling could inhibit cell death-oriented UPR signaling adding to the connection between both molecular machineries. Accordingly, all could inhibit inflammasome activation.

Among the synthesized FST derivatives, some are significantly less cytotoxic towards the cell model employed herein than the parent compound itself. This enabled testing of higher concentrations without deleterious effects, and resulted in the observation of a stronger potential on some or all of the analyzed parameters, being that FST3 was the molecule that displayed the most promising activity.

5. References

1. Chen, L., et al., *Inflammatory responses and inflammation-associated diseases in organs.* Oncotarget, 2017. **9**(6): p. 7204-7218.
2. Karagöz, G.E., D. Acosta-Alvear, and P. Walter, *The unfolded protein response: detecting and responding to fluctuations in the protein-folding capacity of the endoplasmic reticulum.* Cold Spring Harb Perspect Biol, 2019. **3**(11).

3. Yoshida, H., *ER stress and diseases.* The FEBS Journal, 2007. **274**(3): p. 630-658.
4. Libby, P., *Inflammatory mechanisms: the molecular basis of inflammation and disease.* Nutr Rev, 2007. **65**(12 Pt 2): p. S140-6.
5. Grynkiewicz, G. and O.M. Demchuk, *New perspectives for fisetin.* Front Chem, 2019. **7**: p. 697.
6. Khan, N., et al., *Fisetin: a dietary antioxidant for health promotion.* Antioxid Redox Signal, 2013. **19**(2): p. 151-62.
7. Kimira, M., et al., *Japanese intake of flavonoids and isoflavonoids from foods.* Journal of Epidemiology, 1998. **8**(3): p. 168-175.
8. Maher, P., *Protective effects of fisetin and other berry flavonoids in Parkinson's disease.* Food Funct, 2017. **8**(9): p. 3033-3042.
9. Rengarajan, T. and N.S. Yaacob, *The flavonoid fisetin as an anticancer agent targeting the growth signaling pathways.* European Journal of Pharmacology, 2016. **789**: p. 8-16.
10. Imran, M., et al., *Fisetin: An anticancer perspective.* Food Sci Nutr, 2021. **9**(1): p. 3-16.
11. Kashyap, D., et al., *Fisetin: A bioactive phytochemical with potential for cancer prevention and pharmacotherapy.* Life Sci, 2018. **194**: p. 75-87.
12. Ravula, A.R., et al., *Fisetin, potential flavonoid with multifarious targets for treating neurological disorders: An updated review.* Eur J Pharmacol, 2021. **910**: p. 174492.
13. Maher, P., *How fisetin reduces the impact of age and disease on CNS function.* Front Biosci (Schol Ed), 2015. **7**(1): p. 58-82.

14. Elsallabi, O., et al., *Fisetin as a senotherapeutic agent: Biopharmaceutical properties and crosstalk between cell senescence and neuroprotection.* Molecules, 2022. **27**(3).
15. Correia da Silva, D., et al., *A pipeline for natural small molecule inhibitors of endoplasmic reticulum stress.* Frontiers in Pharmacology, 2022. **13**.
16. Lorthongpanich, N., et al., *Fisetin glycosides synthesized by cyclodextrin glycosyltransferase from Paenibacillus sp. RB01: characterization, molecular docking, and antioxidant activity.* PeerJ, 2022. **10**: p. e13467.
17. Jakopin, Ž. and E. Corsini, *THP-1 cells and pro-inflammatory cytokine production: an in vitro tool for functional characterization of NOD1/NOD2 antagonists.* International journal of molecular sciences, 2019. **20**(17): p. 4265.
18. Liu, T., et al., *NF-κB signaling in inflammation.* Signal transduction and targeted therapy, 2017. **2**: p. 17023.
19. Shapouri-Moghaddam, A., et al., *Macrophage plasticity, polarization, and function in health and disease.* Journal of Cellular Physiology, 2018. **233**(9): p. 6425-6440.
20. Chelombitko, M.A., *Role of reactive oxygen species in inflammation: a minireview.* Moscow University Biological Sciences Bulletin, 2018. **73**(4): p. 199-202.
21. Franchi, L., et al., *The inflammasome: a caspase-1-activation platform that regulates immune responses and disease pathogenesis.* Nature Immunology, 2009. **10**(3): p. 241-247.
22. Li, W., et al., *Crosstalk between ER stress, NLRP3 inflammasome, and inflammation.* Applied Microbiology and Biotechnology, 2020. **104**(14): p. 6129-6140.

23. Ding, H., et al., *Fisetin ameliorates cognitive impairment by activating mitophagy and suppressing neuroinflammation in rats with sepsis-associated encephalopathy.* CNS Neuroscience & Therapeutics, 2022. **28**(2): p. 247-258.
24. Chong, W.C., et al., *The complex interplay between endoplasmic reticulum stress and the NLRP3 inflammasome: a potential therapeutic target for inflammatory disorders.* Clinical & Translational Immunology, 2021. **10**(2): p. e1247.
25. Mangan, M.S.J., et al., *Targeting the NLRP3 inflammasome in inflammatory diseases.* Nature Reviews Drug Discovery, 2018. **17**(8): p. 588-606.
26. Dhani, S., Y. Zhao, and B. Zhivotovsky, *A long way to go: caspase inhibitors in clinical use.* Cell Death & Disease, 2021. **12**(10): p. 949.
27. Tanaka, T., M. Narazaki, and T. Kishimoto, *IL-6 in inflammation, immunity, and disease.* Cold Spring Harbor perspectives in biology, 2014. **6**(10): p. a016295-a016295.
28. Yao, C. and S. Narumiya, *Prostaglandin-cytokine crosstalk in chronic inflammation.* Br J Pharmacol, 2019. **176**(3): p. 337-354.
29. Opal, S.M. and V.A. DePalo, *Anti-inflammatory cytokines.* Chest, 2000. **117**(4): p. 1162-1172.
30. Olivari, S., et al., *EDEM1 regulates ER-associated degradation by accelerating de-mannosylation of folding-defective polypeptides and by inhibiting their covalent aggregation.* Biochemical and Biophysical Research Communications, 2006. **349**(4): p. 1278-1284.
31. da Silva, D.C., et al., *Endoplasmic reticulum stress signaling in cancer and neurodegenerative disorders: Tools and strategies to understand its complexity.* Pharmacological Research, 2020. **155**: p. 104702.

32. Iurlaro, R. and C. Muñoz-Pinedo, *Cell death induced by endoplasmic reticulum stress.* The FEBS Journal, 2016. **283**(14): p. 2640-2652.
33. Sano, R. and J.C. Reed, *ER stress-induced cell death mechanisms.* Biochimica et Biophysica Acta (BBA) - Molecular Cell Research, 2013. **1833**(12): p. 3460-3470.
34. Zhang, C., et al., *ATF4 is directly recruited by TLR4 signaling and positively regulates TLR4-trigged cytokine production in human monocytes.* Cellular & Molecular Immunology, 2013. **10**(1): p. 84-94.